immunosensors based on the specificity of antibodies (*16*), most of these sensors rely on exposure of the antibody to subsaturating levels of antigen or to chaotropic agents to restore binding site activity, allowing the sensor to be used more than once. These methods of restoring activity provide discontinuous measurements and less than quantitative recovery. Miller *et al.* (*17*) have developed a reversible sensor based on a similar energy-transfer fluoroimmunoassay that relies on an antibody having a high off-rate, $k_{-1}$, enabling the sensor to respond quickly and reversibly. However, most antibodies have very slow off-rates, making this approach difficult to generalize unless an exhaustive search for a rapid off-rate monoclonal antibody is undertaken for each antigen. With our method this is not necessary—existing immunoassays can be used and coupled to optical fibers through a controlled-release system. The most immediate applications are likely to be in the monitoring of pollutants at toxic waste sites, groundwater aquifers, and agricultural areas where there is pesticide runoff, since antibodies to these analytes are becoming available commercially (Biodesign Inc., Kennebunkport, Maine).


REFERENCES AND NOTES

1. For a recent review, see J. Janata, *Anal. Chem.* **62**, 33R (1990).
2. S. M. Inman, E. J. Stromvall, S. H. Lieberman, *Anal. Chim. Acta* **217**, 249 (1989).
3. F. V. Bright, T. A. Betts, K. S. Litwiler, *Anal. Chem.* **62**, 1065 (1990).
4. R. Bawa, R. A. Siegel, B. Marasca, M. Karel, R. Langer, *J. Controlled Release* **1**, 259 (1985).
5. J. Heller, *Biomaterials* **1**, 51 (1980).
6. G. Kohler and C. Milstein, *Nature* **256**, 495 (1975).
7. A. Nisonoff, *Introduction to Molecular Immunology* (Sinauer Associates, Sunderland, MA, 1985), pp. 29–45.
8. E. Soini and I. Hemmila, *Clin. Chem.* **256**, 353 (1979).
9. C. M. O'Donnell and S. C. Suffin, *Anal. Chem.* **51**, 33A (1979).
10. S. G. Schulman, *Molecular Luminescence Spectroscopy Methods and Applications: Part 1*, P. J. Elung and J. D. Winefordner, Eds. (Wiley, New York, 1985), vol. 77, pp. 1–28.
11. B. J. Tromberg, M. J. Sepaniak, T. Vo-Dinh, G. D. Griffin, *Anal. Chem.* **59**, 1226 (1987).
12. L. M. Christian and W. R. Seitz, *Talanta* **35**, 119 (1988).
13. S. Luo and D. R. Walt, *Anal. Chem.* **61**, 174 (1989). The described method was used to make polymer pieces with a percent degree-of-loading (defined as the dry weight of lyophilized antibody or antigen to dry weight of polymer slab after complete removal of methylene chloride) of 1 to 2% and 8 to 12% for the antibody- and antigen-loaded polymer, respectively.
14. R. Seitz, *CRC Crit. Rev. Anal. Chem.* **19**, 135 (1988).
15. The concentration of unlabeled antigen can be solved by equating the equilibrium equations for reactions 1 and 2

$$K_{eq1} = [\text{F-Ab:Ag}]/([\text{F-Ab}]/[\text{Ag}])$$

$$K_{eq2} = [\text{F-Ab:TR-Ag}]/(\text{F-Ab}][\text{TR-Ag}])$$

and solving for the antigen concentration.

$$[\text{F-Ab}] = [\text{F-Ab:Ag}]/[\text{Ag}]K_{eq1}$$

$$[\text{F-Ab}] = [\text{F-Ab:TR-Ag}]/[\text{TR-Ag}]K_{eq2}$$

Equating the above expressions and solving for [Ag] yields

$$[\text{Ag}] = \frac{[\text{F-Ab:Ag}][\text{TR-Ag}]K_{eq1}}{[\text{F-Ab:TR-Ag}]K_{eq2}}$$

This expression may be rewritten in terms of fluorescence intensities to yield Eq. 3

$$[\text{Ag}] = \frac{([I_{480}/I_{520}][I_{570}/I_{610}])}{([I_{480}/I_{610}] - 0.06[I_{570}/I_{610}])}$$

where $I_x$ is the intensity at $x$ nanometers. The term $0.06[I_{570}/I_{610}]$ is used to correct for the direct excitation of TR-Ag at 480 nm and is determined experimentally.
16. T. Förster, *Faraday Discuss. Chem. Soc.* **27**, 7 (1959).
17. F. P. Anderson and W. G. Miller, *Clin. Chem.* **34**, 1417 (1988).


23 August 1990; accepted 12 November 1990

# High Winds of Neptune: A Possible Mechanism

V. E. Suomi, S. S. Limaye, D. R. Johnson

**Neptune receives only 1/900th of the earth's solar energy, but has wind speeds of nearly 600 meters per second. How the near-supersonic winds can be maintained has been a puzzle. A plausible mechanism, based on principles of angular momentum and energy conservation in conjunction with deep convection, leads to a regime of uniform angular momentum at low latitudes. In this model, the rapid retrograde winds observed are a manifestation of deep convection, and the high efficiency of the planet's heat engine is intrinsic from the room allowed at low latitudes for reversible processes, the high temperatures at which heat is added to the atmosphere, and the low temperatures at which heat is extracted.**

Voyager observations of cloud motions (*1*) showed that Neptune has some of the fastest winds measured on any planet. The strength of Neptune's circulation, despite the small amount of energy received either from its interior or from the sun, was a surprise. Several conceptual models of the general circulation of the giant planets have been proposed (*2*). However, they do not readily provide a simple explanation as to why the highest winds occur on Neptune when the apparent source of energy is so small. Neptune gains only about 1/900th of the solar energy per unit area received by the earth, but the zonal winds in tropical latitudes are more than ten times faster than on the earth.

In this report, we present new measurements of the winds using cloud motions and a new conceptual model based on fundamental principles of angular momentum and energy that offers a plausible mechanism for the exceptionally strong equatorial subrotation or retrograde winds found on Neptune and Uranus. Our model is easiest to illustrate by examination of Neptune's motions in an inertial or absolute frame of reference (Fig. 1).

Gaseous planets are generally assumed to have a core where the fluid rotates as a solid object. Thus, deep within the atmosphere of Neptune we assume that there is a core region where the rotation period equals Neptune's day [assumed to be given by the measurements of the radio period (*3*), 16.11 hours]. Because more energy is received from the interior of the planet than from the sun, deep convective motions develop in the atmosphere as energy is transferred upward from the core region. The upper boundary of the core region represents a surface across which absolute angular momentum is exchanged between the interior and outer gaseous regions of the planet. This same surface as a lower boundary to the free atmosphere determines the vertical extent over which reversible isentropic processes may occur.

An estimate of the upper boundary of the core region can be obtained from the observed cloud motions and a parameter called the potential radius. The potential radius is the perpendicular distance from the axis of rotation at which the relative zonal motion of a given cloud feature vanishes through virtual radial displacement under angular momentum conservation, that is, where the periods of rotation for the planet and the displaced cloud become equal. For all latitudes where the rotation period of a cloud exceeds that of the interior, the potential radius is closer to the spin axis, whereas for all latitudes where the rotation period is less than that of the deep interior, the potential radius is located farther from the spin axis.

We have calculated the meridional distribution of the potential radii for the measured cloud motions (*4*) (Fig. 2). In the

Space Science and Engineering Center, University of Wisconsin–Madison, 1225 West Dayton Street, Madison, WI 53706.

equatorial region, the potential radii form a quasi-cylinder some 2000 to 3000 km below the visible surface. The quasi-cylindrical form of the potential radius indicates that to a first approximation, the spatial distribution of angular momentum is uniform. In contrast, at mid- to high latitudes, the potential radii nearly match that of the visible surface. These data indicate that the atmospheric vorticity and the local planetary vorticity of solid rotation are nearly equal at high latitudes. Evidently, there are two different dynamical regimes separated by a transition zone.

If our conceptual model is valid we can expect that the lower interface has irreversible heat transfer processes because of conduction and possible hydromagnetic effects at the lower boundary. Similarly we can expect that large irreversible heat transfer processes occur in the atmosphere's upper regions by radiation. Between these two levels at low latitudes we can expect a deep region of reversible processes.

For an adiabatic lapse rate of 0.8 K/km, the temperature at the lower boundary is more than 1000 K. If convection starts at these depths, then the Brayton cycle engine efficiency given by $1 - [T\ (\text{top})/T\ (\text{bottom})]$, where $T$ is temperature, is about 1 − 60/1000 or 94%. A Brayton cycle is one where the heat gains and the heat losses occur at constant pressure at the bottom and at a different but constant pressure at the top. On Neptune these vertical differences for both temperature and pressure are large. It is the deep vertical extent of the convection and the extreme low temperature at which heat losses occur in concert with mainly reversible isentropic processes above the potential radius that provides for the high efficiency needed to maintain the high wind regime against irreversible processes.

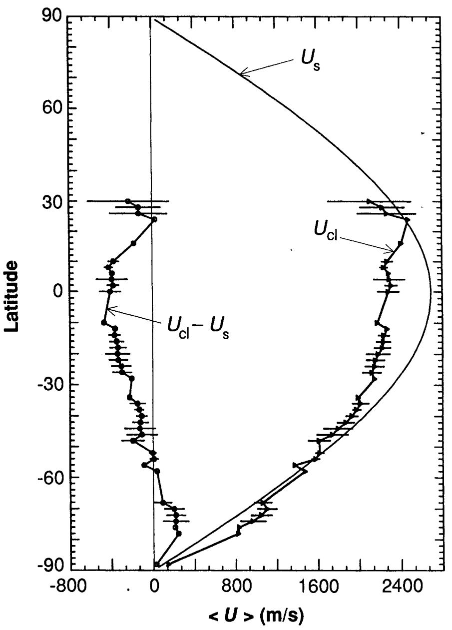


**Fig. 1.** A meridional distribution of Neptune's average cloud zonal velocities ($U_{cl}$) in an absolute frame (triangles), the zonal velocity of Neptune's visible surface ($U_s$) as if it were rotating as a solid body (solid line), and the relative zonal velocity ($U_{cl} - U_s$) in a frame of reference rotating with the measured radio rotation rate (circles) from recent measurements (4). The error bars represent 1 rms deviation about the average of the measured vectors in a given latitude band and mostly reflect variability, as the measurement errors (excepting misidentification of the target) are generally much smaller.

In the region of permitted reversible processes we assume that to a first approximation the total flow energy (TFE) being conserved under steady isentropic motion is defined by

$$\text{TFE} = \text{enthalpy} + \text{gravitational energy}$$
$$+ \text{kinetic energy} = \text{constant}$$

This condition provides for reversibility of energy exchange under cyclic processes and is an application of the laws of thermodynamics, as described by Tolman and Fine (5) generally, and recently applied by Johnson (6) to Earth's circulation. We assume that Neptune's atmosphere has regions of volume expansion and contraction involving cyclic processes where reversible processes take place in Hadley-like circulations and are represented by the combination of steady convection within vertical branches and meridional branches demanded by mass continuity. Although entropy is being generated by irreversible processes, important reversible processes dominate in the vertical branches.

The region above the potential radius extending meridionally between 54° north and south and vertically several thousand kilometers below the visible surface provides plenty of room for both reversible and irreversible processes. Thus, the lower the potential radii relative to the visible surface, the more room vertically and meridionally for Hadley-like circulations to form. Thus, the deeper the core, the more efficient the atmospheric heat engine that maintains the high winds can be.

Energy emanating from the planets' interior, the convective buoyancy of fluid elements, and reversible processes maintain the supply of kinetic energy against frictional dissipation. In polar latitudes the sense of buoyancy is oriented along planetary angular momentum surfaces, perpendicular to its meridional gradient in angular momentum. The hydrodynamic stability from the meridional gradient of angular momentum (7) imposes a severe constraint to meridional displacement; thus, the deep convection primarily transports internal energy upward along surfaces of angular momentum without meridional motion. This situation allows the atmosphere to assume a local value of planetary vorticity characteristic of solid rotation. In contrast, in equatorial latitudes, the sense of convective buoyancy is oriented perpendicular to the hypothetical cylindrical surfaces of planetary angular momentum. However, there are few constraints on vertical and horizontal motions because the circulation is free to adjust to a uniform value of angular momentum that is determined by frictional coupling at the core-atmosphere interface and the exchange of angular momentum implicitly involved with reversible processes. Convection in equatorial regions thus creates a region of relatively uniform angular momentum; and the potential radius, the easterlies of tropical latitudes, and the westerlies in mid-latitudes are all a reflection of this exchange. The latitude where the potential radius intersects the visible surface of the planet marks the transition between the two dynamical regions.

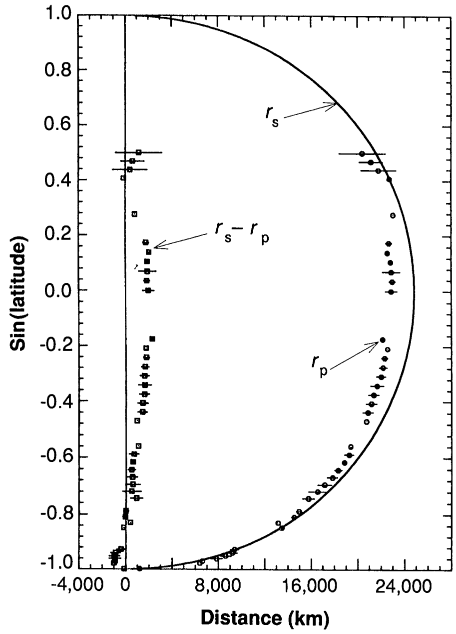


**Fig. 2.** Potential radius ($r_p$) of observed cloud motions on Neptune (circles) shown as a function of the sine of the latitude. The corresponding depth ($r_s - r_p$) below or above the visible surface ($r_s$) of Neptune is shown on the same scale by the boxes.

In an axially symmetric, frictionless system, absolute angular momentum is conserved. Any meridional displacement on a geopotential surface under such conditions will change the intensity of the east-west flow as the distance normal to the spin axis changes. Easterly winds in equatorial regions can be maintained by meridional motion along geopotential surfaces from higher latitudes under the conservation of absolute angular momentum. On a gaseous planet with a deep convective atmosphere, the motions are not restricted to meridional displacements along geopotential surfaces. A change in the radial distance from the axis of rotation can be accomplished by both meridional motions along the surface and by radial motions normal to geopotential surfaces.

Several features characterize the atmospheric region where reversible energy exchange and large radial displacements occur. In an inertial reference frame, east winds will have less absolute kinetic energy than equally strong west winds. Should a parcel be displaced upward through a layer near the equator it would, because of conservation of angular momentum, lose kinetic energy. Because total flow energy must be conserved in this process, a repartitioning of energy in the region of reversible processes occurs, as described below.

For two different latitudes, consider idealized vertical displacements of parcels from a geopotential surface deep down to another surface higher up under the conservation of total flow energy and angular momentum. A geopotential surface is a level of equal potential energy of a unit mass by virtue of its position in the field of gravity. With upward displacement of a parcel at the equator, the geopotential energy increases from a mutual decrease of absolute kinetic energy and enthalpy. With a similar vertical displacement of a parcel at the pole, the geopotential energy increase stems solely from the enthalpy decrease because the kinetic energy remains the same. As a result, the decrease of enthalpy at the equator is less than at the pole. From these idealized vertical displacements and a uniform meridional distribution for each of the components of energy at the core-atmosphere interface, it follows that upper atmospheric temperatures on the same geopotential surface would be warmer over equatorial latitudes than over polar latitudes even without any external energy input such as the heating from the sun.

Another implication is illustrated by the case of an air parcel rising from deep layers over the equator. The parcel would flow westward and produce strong easterly winds in tropical latitudes on each side of and over the equator. Westerlies would develop at the poleward extent of the tropical regime of uniform angular momentum because of meridional exchange within an axially symmetric circulation.

This model can also account for circulation in Neptune's Great Dark Spot (GDS). For example, assume that same vertical motion occurs at 20°S over an area above the same size as the GDS. Westward flow would form in the upper layers. Presumably, as the rising current encounters the tropopause, horizontal divergence of the air parcels would result in anticyclonic circulation. That is what appears to happen in the GDS (*1*). The GDS could also be a giant vortex on its own, acting as the primary means to transport heat and angular momentum upward. Indeed the symmetry of the wide cloud band observed in the low latitudes about the GDS rather than the equator is a suggestion that that is the case. Upward flow in the tropics could be in the form of a classical Hadley cell flow, a giant hot tower, or more likely, a combination. If the base of the vortex for the GDS is at the level of the potential radii, the relatively uniform angular-momentum values of the easterlies at the visible surface of the planet would be accounted for within the vortex through transfer of angular momentum by pressure stresses within the belt of equatorial easterlies during the prolonged ascent of the parcels.

Although the Great Red Spot (GRS) on Jupiter and the GDS on Neptune appear to be similar giant vortices, there is an important difference. The period of the GRS practically matches that of the planet's radio rotation rate, drifting westward at approximately 4 m/s, sometimes slightly faster, sometimes slower by as much as 1 m/s. On the other hand Neptune's GDS moves rapidly to the west at a period of 18.3 hours compared to the interior period of 16.11 hours. This difference between them might indicate that the GRS is shallow and the GDS is deep. Furthermore, for the easterlies on Jupiter and also on Saturn, the potential radii surfaces lie much closer to the visible surface than on Neptune or Uranus.

Uranus, most similar to Neptune in size, displays an atmospheric circulation somewhat similar to that of Neptune and a comparable rotation period (*3*). Uranus appears to have a superrotating atmosphere poleward of about 20°S and a subrotating atmosphere equatorward of that latitude, whereas Neptune has a subrotating atmosphere in a wider belt approximately between $\pm 54°$ latitude. On Uranus we can expect that the quasi-cylindrical surface defined by the potential radius will intersect the visible surface of the planet at $\pm 20°$ latitude. As the depth of the potential radius below the visible surface of Uranus at the equator is considerably less than that compared to Neptune, the difference between the temperature at this depth where heat is added and the temperature at the upper level where heat is extracted is also less than that on Neptune. Such a structure would lead to a less efficient heat engine and could be the reason why Uranus has slower winds compared to Neptune. The radii of these quasi-cylindrical surfaces are different on Uranus and Neptune because Neptune transfers more energy from its interior and thus supports deeper convection compared to Uranus.

Tassoul (*9*) describes three theories to account for the differential rotation in stars and cautions that "no commonly accepted model exists at the present time." (In a sense the outer planets with internal heat sources could be considered as "cold stars" since they lose more heat by radiation than they gain from the sun.) In one, the sense of the mean meridional circulation is determined by the anisotropic eddy viscosity in the convective zone. Anisotropic eddy viscosity with greater transverse than radial values forces axially symmetric mean circulations in each hemisphere; the flow rises at the poles and moves toward the equator at the outer boundary, then streams back to the poles on the inner boundary of the convective shell. The net angular momentum transport by the mean circulation in each hemisphere is toward the equator and leads to equatorial superrotation such as observed on the sun, Jupiter, and Saturn. With greater radial than transverse anisotropic eddy viscosity values, a reversal of the meridional circulations occurs that provides for subrotation in the equatorial zone. On Neptune, the greater apparent radial eddy viscosity should extend over many scale heights in the equatorial zone.

If this theory holds for the outer planets, one must find a process that changes orthogonally the direction of anisotropy for Jupiter and Saturn compared to Uranus and Neptune. On rotating gaseous bodies with their wide range of scales of motion, different dynamical structures control their eddy viscosities. In an equatorial annulus of uniform angular momentum where reversible processes are permitted, neutral vertical stability occurs on a global scale within the volume. However, in this zone, a measured lapse rate in a direction parallel to the axis of rotation is equal to the lapse rate for an ordinary neutral adiabatic process whereas a different cylindrical surface will have a smaller measured lapse rate and would appear to be stable to small-scale vertical motions. This effect is more than a factor of 10 greater on Jupiter and Saturn, because of their greater rotation rates and radial size, than on Uranus and Neptune. Would this effect be large enough to change orthogonally the direction of anisotropy on Jupiter and Saturn compared to Uranus and Neptune? If so, a reduced radial eddy viscosity could result in equatorial superrotation, a shallower layer of reversible processes, and reduced top and bottom temperature differences and lead to a less efficient set of planetary engines.

REFERENCES AND NOTES

1. B. A. Smith *et al.*, *Science* **246**, 1422 (1989); H. B. Hammel *et al.*, *ibid.* **245**, 1367 (1989).
2. A. P. Ingersoll, *ibid.* **248**, 308 (1990).
3. J. W. Warwick *et al.*, *Science* **246**, 1498 (1989).
4. S. S. Limaye, L. A. Sromovsky, V. E. Suomi, *Adv. Space Res.*, in press. All narrow-angle frames between 3 and 6 days before encounter (FDS #s 11215.36 to 11305.00) in different filters were used for the measurements of cloud motion. Targets were followed for as long as possible, and linear drift rates were obtained by regression from multiple position and time measurements. Resulting vectors were binned in latitude bands and averaged. The error bars represent ±1 rms deviation within the latitude band.
5. R. C. Tolman and P. C. Fine, *Rev. Mod. Phys.* **20**, 51 (1948).
6. D. R. Johnson, *Adv. Geophysics* **31**, 43 (1989).
7. A. Eliassen, *Astrophys. Norv.*, **5**, 19 (1951).
8. This argument presumes that the time scale of Lagrangian convective transport within the vortex is small relative to the period of vortex rotation.
9. J. L. Tassoul, in *Theory of Rotating Stars* (Princeton University Press, 1978), p. 506.
10. This work was supported by National Aeronautics and Space Administration (NASA)–Jet Propulsion Laboratory contract 957739, NASA grant NGR 189-50-002 from the Planetary Atmosphere Program and NASA grant NAG5-81. We thank F. Bretherton, L. Sromovsky, H. Revercomb, and J. Anderson for discussions as well as an anonymous referee for comments.

4 October 1990; accepted 2 January 1991

# Nylon Production: An Unknown Source of Atmospheric Nitrous Oxide

MARK H. THIEMENS AND WILLIAM C. TROGLER

**Nitrous oxide in the earth's atmosphere contributes to catalytic stratospheric ozone destruction and is also a greenhouse gas component. A precise budgetary accounting of $N_2O$ sources has remained elusive, and there is an apparent lack of source identification. One source of $N_2O$ is as a by-product in the manufacture of nylon, specifically in the preparation of adipic acid. Characterization of the reaction $N_2O$ stoichiometry and its isotopic composition with a simulated industrial adipic acid synthesis indicates that because of high rates of global adipic acid production, this $N_2O$ may account for ~10 percent of the increase observed for atmospheric $N_2O$.**

NITROUS OXIDE IN THE EARTH'S atmosphere is known to be increasing by about 0.2% per year (*1, 2*), presumably from anthropogenic activity. Although the absolute concentration of nitrous oxide is relatively low [~300 parts per billion by volume (ppbv)], it may influence global climatic processes as a result of one of its stratospheric thermal removal reactions:

$$N_2O + O\,(^1D) \rightarrow NO + NO \quad (61.7\%) \quad (1)$$

$$\rightarrow N_2 + O_2 \quad (38.3\%) \quad (2)$$

The stratospheric loss rate for reaction 1 is $1.1 \times 10^8$ to $1.9 \times 10^8$ molecules $cm^{-2}\,s^{-1}$, and the total loss rate, including photolysis, is $0.9 \times 10^9$ to $1.4 \times 10^9$ molecules $cm^{-2}\,s^{-1}$ (*3*). Nitrous oxide serves as the major stratospheric source of NO, which is unambiguously implicated in catalytic ozone destruction. Second, it is a recognized greenhouse gas that may in the future contribute to an enhanced greenhouse effect by as much as 10% (*4*). Unlike most other trace greenhouse gases and $O_3$ destructive agents, $N_2O$ does not have an adequately resolved budget. About 30% of the sources have not been identified (*5*). Because of its atmospheric lifetime of approximately 150 years (*6*), identification of all significant sources is particularly important. There are other features of the global $N_2O$ budget that are problematic. The rate of increase of $N_2O$ levels is ~0.9 ppb $yr^{-1}$ in the Northern Hemisphere and 0.7 ppb $yr^{-1}$ in the Southern Hemisphere (*2*). In the Northern Hemisphere, $N_2O$ concentrations are typically 0.8 ppbv higher from April to June than during the rest of the year, possibly because of a large, though undefined, continental anthropogenic source (*2*). A clear resolution of the reason for the hemispheric $N_2O$ difference or seasonality is needed.

With regard to identification of atmospheric trace species, sources, sinks, and transformation mechanisms, stable isotope ratio measurements can provide useful, diagnostic information. For atmospheric $N_2O$ there is, at present, a limited database for the isotope ratios $\delta^{15}N$ (*7–10*) and $\delta^{18}O$ (*10–12*). Nitrogen isotopic measurements reveal that $N_2O$ in maritime air differs from continental air (*8*) and is somewhat variable. This suggests variable source strengths. The processes that determine the ultimate nitrogen and oxygen isotopic composition of $N_2O$ in the ocean have not been identified unambiguously. Denitrification has generally been presumed to be the source of $N_2O$ with high $^{15}N/^{14}N$ and $^{18}O/^{16}O$ ratios (*9, 11–13*); however, recent simultaneous $\delta^{15}N$ and $\delta^{18}O$ measurements of Pacific oceanic $N_2O$ profiles suggest that the opposite is the case (*10*). The heavy isotopes in oceanic $N_2O$ are depleted, relative to atmospheric $N_2O$ to depths of about 600 m, but significantly enriched in deep and bottom waters. Kim and Craig (*10*) proposed that deep $N_2O$ production by nitrification is simultaneously coupled to a kinetic isotopic fractionation during bacterial respiration, and that this process results in an overall enrichment of heavy isotopes in $N_2O$. Oceanic regions where denitrification occurs, for example, the eastern equatorial Pacific, are also sites of upwelling and thus can provide a source of $N_2O$ (*14–16*) isotopically similar to tropospheric $N_2O$ (*9*). As concluded by Kim and Craig (*10*), isotopic definition of $N_2O$ in active upwelling sites is needed; in consideration of present uncertainties in the atmospheric $N_2O$ budget (*5*), identification of all significant $N_2O$ sources with concomitant isotopic measurements is needed.

On first consideration one might conclude that industrial sources of $N_2O$ are insignificant because of its minor usage (*17*). Its chief application, as a nontoxic propellant in canned whipping cream, does not constitute a significant atmospheric pollution source. In this report, we call attention to an industrial source of $N_2O$ that has atmospheric significance. Nitrous oxide is a by-product in the manufacture of monomers for 6,6- and 6,12-nylon. In 1989 $1.24 \times 10^9$ kg of nylon were produced in the United States alone (*18*). Nylon polymers have typically been formed by condensation polymerization of a dicarboxylic acid and diamine. The most widely used diacid, adipic acid, is prepared primarily by air oxidation of cyclohexane to cyclohexanol-cyclohexanone mixtures, followed by oxidation with $N_2O$ to adipic acid (*19*). In 1989, U.S. production of adipic acid totaled $7.44 \times 10^8$ kg (*18*). Because western European and Japanese production essentially equals U.S. production (*19*), we might assume that other world sources, such as China, the Soviet Union, and Eastern Europe have a total adipic acid output comparable to the United States This suggests a 1989 worldwide production of $2.2 \times 10^9$ kg of adipic acid, which agrees with an estimate of $2.2 \times 10^6$ tons, or $2.0 \times 10^9$ kg worldwide for 1983 (*20*). We have focused on the nitric acid oxidation step involved in adipic acid synthesis because it results in the stoichiometric production of $N_2O$ on a large scale.

Most earlier workers have reported indeterminate stoichiometries for the $N_2O$ produced by the nitric acid oxidation of cyclohexanol-cyclohexanone mixtures, as shown in Eq. 3.

Department of Chemistry, University of California, San Diego, La Jolla, CA 92093.